Film bulk acoustic resonator oscillator based humidity sensor with graphene oxide as the sensitive layer

Weipeng Xuan,[1] Marina Cole, [2] Julian W. Gardner,[2] Sanju Thomas, [2] Farah-Helúe Villa-López,[2] Xiaozhi Wang,[1] Shurong Dong,[1] Jikui Luo,[1,3]

[1] College of Information Science & Electronic Engineering, Zhejiang University, Hangzhou, China, jackluo@zju.edu.cn

[2] Microsensors and Bioelectronics Laboratory, University of Warwick, Coventry, United Kingdom, Marina.Cole@warwick.ac.uk

[3] IMRI, University of Bolton, Bolton, United Kingdom,

Abstract: Film bulk acoustic wave resonator (FBAR) is a type of resonators with high frequency and small dimension, particularly suitable to be sensors for physical and biochemical sensing with high sensitivity. FBAR based sensors have been extensively studied, but most of them use discrete devices and network analyzer for evaluation, thus they are far from practical application. This paper reports the design and analysis of a FBAR-based Pierce oscillator and a FPGA based frequency counter, and use of the oscillator as a humidity sensor with the frequency counter as the measuring circuit. Graphene oxide (GO) is used as the sensitive film to improve the sensitivity. The resonant frequency of the oscillator with a GO film shows a linear decrease with increase in relative humidity with a sensitivity of *ca.* 5 kHz per %RH (relative humidity) in the range of 3%RH to 70%RH, and a higher frequency shift is induced above 70%RH. The FBAR oscillator sensor shows excellent stability and repeatability, demonstrating the feasibility and potential sensing application using the integrated FBAR chip and simple frequency counter, particularly suitable for portable electronics.

Keywords— FBAR, Pierce oscillator, humidity sensor, graphene oxide.

1. Introduction

Humidity is a dynamic and important variable in various fields of industry, agriculture and human activities. Humidity sensors based on changes in capacitance[1] and resistance[2] of devices have been extensively investigated using porous materials or polymers as the sensing films. Acoustic wave resonators such as quartz crystal microbalance (QCM), surface acoustic wave (SAW) and film bulk acoustic resonator (FBAR) have also been utilized to develop humidity sensors. QCM-based humidity sensors received considerable attentions due to the advantage of matured technology and reasonably high sensitivity [3, 4], and SAW humidity sensors have been developed using polymers or graphene oxide (GO) as the sensing layer [5, 6]. As FBAR devices typically work at high frequency range of a few GHz, the induced frequency shifts of FBAR sensors by any variation will be much larger than those of QCMs and SAW sensors, improving the sensitivity of the sensors significantly. Furthermore FBARs are small in size compared to SAW and QCM sensors, they are particularly suitable for integration with CMOS circuit for sensing applications. As such, FBARs have been utilized for various sensor developments. FBAR humidity sensor without any sensing film was reported [7], though this type of sensors showed nonlinearity for humidity response. Although substantial progress has been made in developing high sensitivity acoustic humidity sensors, so far, most of the researchers used discrete acoustic resonators for investigation, and the performances of the humidity sensors were characterized using network analyzer [8, 9], far from practical application. For application, chip-type sensors and the corresponding integrated electronics for measuring frequency shift and signal processing are necessary, but limited work has been done in this aspect, not even to mention that chip-type sensors with nanomaterials as the sensitive layers.

Since FBARs have many excellent properties such as high quality factor, high frequency and low power consumption, they have been extensively utilized to develop oscillators [10, 11] with different circuit topologies for various applications. A low power FBAR pierce oscillator based on 0.18 μm CMOS with a frequency of 1.9 GHz was designed by Otis et al [11], and a colpitts topology FBAR oscillator with temperature compensation by Pang et al[12]. A bulk acoustic wave (BAW)-tuned quadrature VCO using differential oscillator circuit topology was reported by Rai et al[13], and a BAW resonator-based 2.4 GHz receiver by Heragu et al[14]. Flatscher designed a BAW-based transceiver for tire-pressure sensor with a phase noise of -112.17dBc/Hz@100kHz. The phase noise is one of the most important parameters used to evaluate the performance of an oscillator, especially for sensing application as it affects the detection limit.

Although many FBAR-based oscillators have been developed, FBAR oscillator has not been utilized as a humidity sensor. In this work, a FBAR-based oscillator using the Pierce structure design and a FPGA based frequency counter are developed for humidity sensing, as a step towards miniaturisation and monolithic implementation of FBAR sensors. FBARs with a working frequency of 1.25 GHz are fabricated and used in designing the FBAR oscillators. Meanwhile, a frequency counter based on FPGA and a PC based data acquire software are developed for precision measurement of frequency and measurement control. Results show that the output frequency of the oscillators is indeed determined by the resonant frequency of the FBAR devices used[13], the sensitivity could be improved by using a GO sensing film, and the oscillator chip and control electronics perform well. The research demonstrates the potential of the integrated oscillator humidity sensor for practical application that have a very small dimension, low power consumption and digital frequency output, particularly suitable for portable electronics such as mobile phones.

2. Experimental and oscillator design

2.1 FBAR device and MBVD model

The FBAR devices used in this work are a three-layer, back-trench structure with top and bottom aluminum electrodes sandwiching a (0002) oriented piezoelectric Zinc Oxide (ZnO) layer. It was fabricated on a SiO_2/Si substrate. Figure 1(a) shows the microfabrication process for the FBAR devices: (a1) a double-side polished silicon wafer was washed with acetone, ethanol, and deionized (DI) water in sequence and finally dried by nitrogen gas; (a2) a 200 nm thick aluminum (Al) layer was deposited by direct current sputtering method, patterned by photolithography and etched to form the bottom electrodes of FBARs; (a3) a ~1.5 μm thick ZnO piezoelectric film was deposited by reactive sputtering; (a4) it was then patterned and etched using a diluted HCl solution to form the vias to expose the bottom electrodes; (a5) a 200 nm thick top aluminum layer was deposited by direct current sputtering method and patterned to form the top electrodes of FBARs; (a6) the back side silicon was patterned and removed by deep reactive ion etch, with the SiO_2 (~1 μm thickness) membrane as the etch-stopper as well as the support layer of the FBARs.

Once fabricated, the S-parameters of the devices were assessed using a network analyzer (Agilent E5071C), and the Modified Butterworth-Van Dyke (MBVD) equivalent circuit was extracted [15] which is needed for the oscillator design and analysis. Figures 1(b)-1(d) show the fabricated FBAR, S-parameters with a resonant frequency of 1247 MHz and the corresponding MBVD circuit, respectively. In this MBVD circuit model, C0 is the static capacitance of the FBAR device, and the arm containing Rm, Lm, and Cm is the "motional arm" of the MBVD circuit, which arises from the mechanical vibration of the FBAR. R0 and Rs represent loss of the device. All these values of the parameters were extracted from S-parameters obtained by network analyzer.

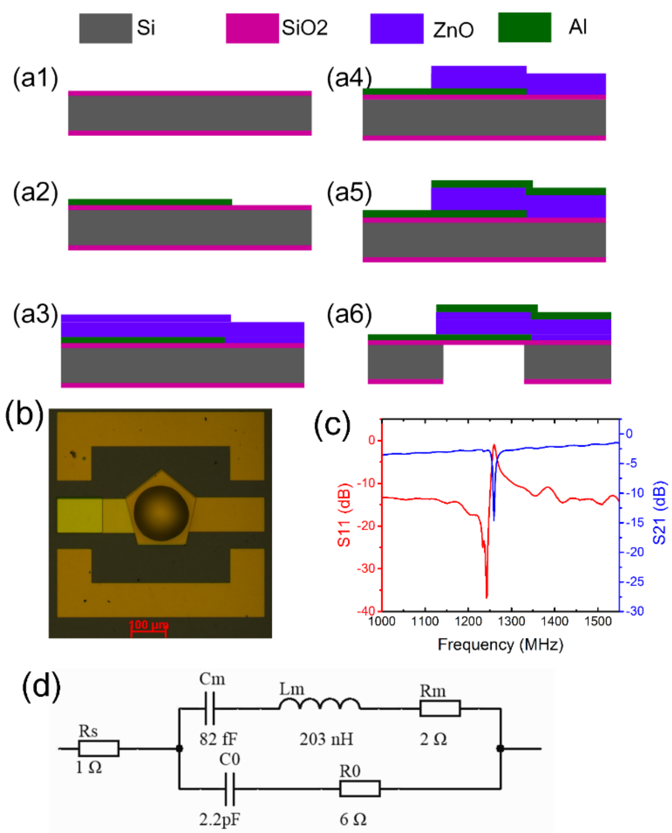

Figure 1. The FBAR microfabrication process (a): (a1) a silicon wafer with a ~1um SiO2 film, (a2) shape bottom electrode, (a3) deposited ZnO, (a4) exposed the bottom electrode, (a5) graphic top electrode, (a6) etch the back side silicon. Microphoto image of the fabricated FBAR device (b), the obtained S-parameters of the device (c), and the MBVD model circuit and specific values of variables extracted from the S-parameters (d).

2.2 Pierce oscillator design implementation

The Pierce FBAR oscillator circuit is shown in figure 2(a). To achieve oscillation for the oscillator, the Barkhausen criteria needs to be satisfied as follows,

$$|\mathrm{AF}| \geq 1 \text{ and } \angle\mathrm{AF} = \mathrm{n} * 2\pi. \quad (1)$$

Where A is the gain of the amplifier and F is the gain of the feedback circuitry. In the circuit design, the low noise silicon bipolar RF Transistor BF93A (Infineon Technologies AG), which has a transition frequency of 6 GHz, was used as the amplifier. The FBAR device (effective area about 500 μm^2), capacitor C1 and C2, compose the feedback circuitry; the resistors, R1 and R2, provide the DC bias for the transistor. The impedance of the MBVD circuit of the FBAR is given by,

$$\mathrm{Z} = \mathrm{Rs} + \left(\frac{1}{sC0} + R0\right) \parallel \left(\frac{1}{sCm} + sLm + Rm\right) \quad (2)$$

As shown in figure 2(b), the impedance of the FBAR device has two peaks, the first peak is determined by the motional arm, $\mathrm{fs} = \frac{1}{2\pi\sqrt{Cm \times Lm}}$, called the series resonant frequency, and the second one is $\mathrm{fp} = \frac{1}{2\pi\sqrt{C \times Lm}}$, $(C = \frac{C0 \times Cm}{C0 + Cm})$, called the parallel resonant frequency. As it can be seen from figure 2(c), there are two different frequencies with zero degree phase shift for the oscillator closed loop. The gain of the oscillator should be larger than the unit to fulfill the oscillating condition. The oscillator circuit was simulated using the real parameters of the components and extracted parameters of the FBAR, with the results shown in figures 2(c) & (d). Two frequencies with zero phase shifts were obtained, one near 1247 MHz with a gain near 2, and the other one at 1301 MHz with a gain near zero, implying that the oscillator could only oscillate at the frequency near 1247 MHz. The output spectrum of the oscillator with a 5 V power supply is shown in figure 2(d), with the fundamental frequency of 1247 MHz, and the output power of 7 dBm.

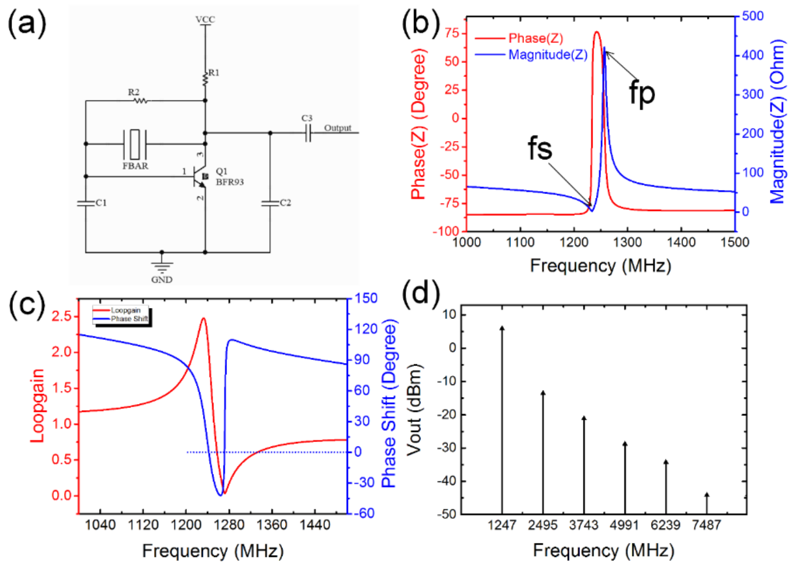

Figure 2. (a) The oscillator structure, (b) the impedance of the FBAR device, (c) the closed loop gain and phase shift of the pierce oscillator, and (d) the simulated output spectrum of the oscillator circuit.

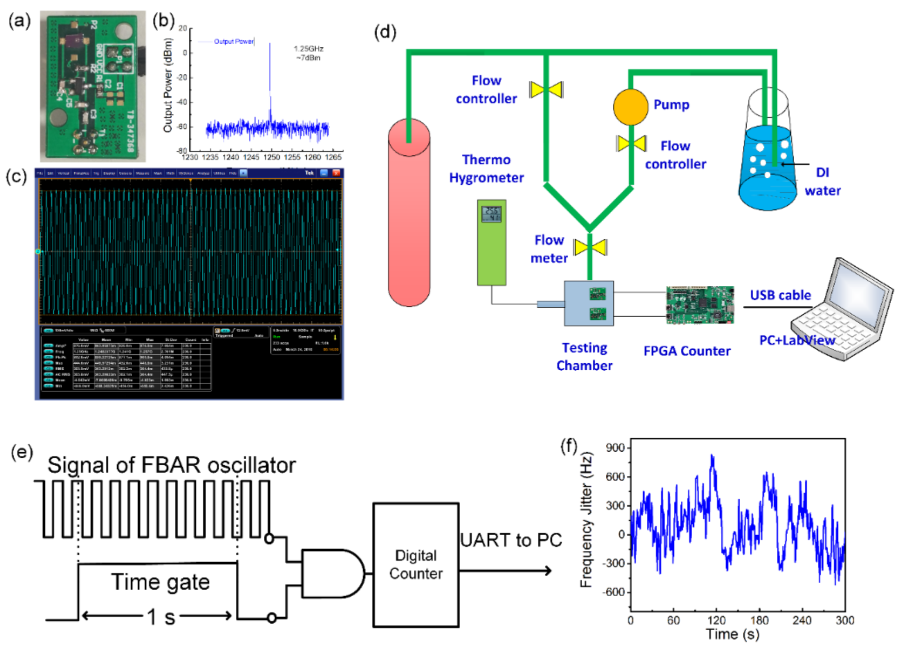

Figure 3. (a) The FBAR oscillator board, (b) the output spectrum of the Pierce oscillator, (c) the output signal of the oscillator, (d) the sensor testing plarform, (e) the frequency counter block, and (f) the frequency jittter obtain by the frequency counter developed.

The oscillator circuit board developed is shown in figure 3(a) with the FBAR device wire-bonded to the PCB board. The 50Ω impedance matching factor was considered in designing the PCB board. A Tektronix MDO3012 Mixed Domain Oscilloscope was used to characterize the fabricated oscillator. The output spectrum of the oscillator fabricated is illustrated in figure 3(b). The output power of the fundamental frequency of the oscillator chip is ~7 dBm with a 5 V power supply, consistent with the simulation result shown above. Figure 3(c) shows the measured output signal of the oscillator using a Tektronix DPO5204B digital phosphor oscilloscope.

2.3 The sensor preparation and setup of the sensing experiments

Use of a sensitivity sensing layer could improve the performance of a sensor[6]. To develop the high sensitivity FBAR oscillator humidity sensors, a GO layer was used as the sensing layer in this work. The GO solution was purchased from C6G6 Company, with a concentration of 14.6 mg/ml. The solution was diluted 100 times using DI water and used for thin GO film deposition on the surface of FBAR devices. Before the GO film deposition, the FBAR device was rinsed with ethanol and DI water, then dried using nitrogen gas and baked in an oven for 2 hours at 60 ^{o}C. The GO film was dip coated on the surface of the devices by placing the device horizontally into the diluted solution for a while, and then pulled out. The thickness of GO layer can be controlled by varying the deposition time (from 30 to 90 sec for different samples). GO is composed of hydrophobic carbon six-membered rings layer and a large number of hydrophilic groups (such as hydroxyl, carboxyl) bonded to carbon layer, the characteristics of the GO material was reported previously [16]. After GO film deposition, the FBAR was wire-bonded to the oscillator board and placed in the test chamber for humidity sensing. Two oscillators were placed into a test chamber (volume about 160 ml), one with a bare surface FBAR as a reference and one with a GO-coated FBAR for sensing. Humidity in the test chamber was controlled by changing the ratio of dry and wetted nitrogen, as shown in figure 3(d). The FPGA based frequency counter (shown in figure 3(e)) was connected to the oscillator to measure the frequency shift, and a PC was connected to the frequency counter to record the frequency shift. Figure 3(f) shows the frequency jitter (noise) of the sensor in time domain obtained by the frequency counter with a value about 1 kHz. Additional information for sensing experiments could be found from our previous publication [16].

3. Sensing results and discussion

3.1 FBAR mass loading sensor

The sensing mechanism of the FBAR oscillators is believed to be the same as that of the discrete FBAR sensor, i.e. the mass loading effect as the resonator frequency of the oscillator is determined by that of the FBAR. Sauerbery first developed a relationship between the change in resonance frequency and an added mass for a resonator as [17],

$$\Delta f = -\frac{2f_0^n}{A\sqrt{\rho_q \mu_q}}\Delta m \tag{4}$$

where Δf and f_0 are the frequency shift and the original resonant frequency of the resonator (FBAR in this work) respectively, ρ_q and μ_q are the density and the shear modulus of the piezoelectric material, A is the active area of the sensor and Δm is the added mass. Since the electrode thicknesses in FBARs are relatively thicker, compared to those in QCMs and SAWs, the sensitivity of the FBAR sensor ($\Delta f/\Delta m$) is typically not proportional to the square of resonant frequency, but with 1<n<2. Since FBARs have much higher frequency, they have much higher sensitivities compared to those of QCMs and SAWs. The equation also indicates that Δf is linearly correlated to the added mass Δm for the resonator. The mass sensitivity per area of the sensor could be defined as,

$$\alpha = \frac{A*\Delta f}{\Delta m} \tag{5}$$

From equation (4), we obtain the mass sensitivity of about 800 Hz/(ng/cm^2) for our bare surface FBAR device assuming n=2. After the deposition of GO film, the frequency of the oscillator was found to decrease by about 5 MHz due to the mass loading effect, which corresponds to a GO film thickness of about 50 nm for this device.

3.2 Real-time humidity sensing

Figure 4(a) shows the real-time frequency responses of the two oscillators to the variation of relative humidity, one with a bare surface FBAR and other with a 50 nm GO coated FBAR, measured by the frequency counter developed. Before introducing wetted nitrogen gas, the sensors in the chamber were purged with dry nitrogen gas for sufficient time to obtain a stable baseline. The flow rate for wetted nitrogen was then varied to change the humidity in the chamber, but the total flow rate of gases (dry and wetted nitrogen gases) was fixed at 500 sccm. Nine sensing cycles were performed for this experiment with one cycle comprised of water absorption (wetted nitrogen) and desorption (dry nitrogen purge) processes. Once the moist gas is introduced, the oscillating frequency starts to decrease due to the water molecules adsorption onto the surface of the FBAR device. When the gas is switched to dry nitrogen, the resonant frequency recovers gradually due to desorption of water molecules from the surface of FBAR. As shown in figure 4(a), the absorption-desorption process of water molecules is reversible, i.e. the resonant frequency of the oscillator sensor returns to its original baseline once a dry gas is switched on for sufficient time; and it also shows that the frequency shift increases with the increase of humidity. The oscillator with a GO sensing layer FBAR has larger frequency shift than the one with a bare surface FBAR, indicating that GO film enhances the absorption of the water molecules as reported for SAW sensors [4].

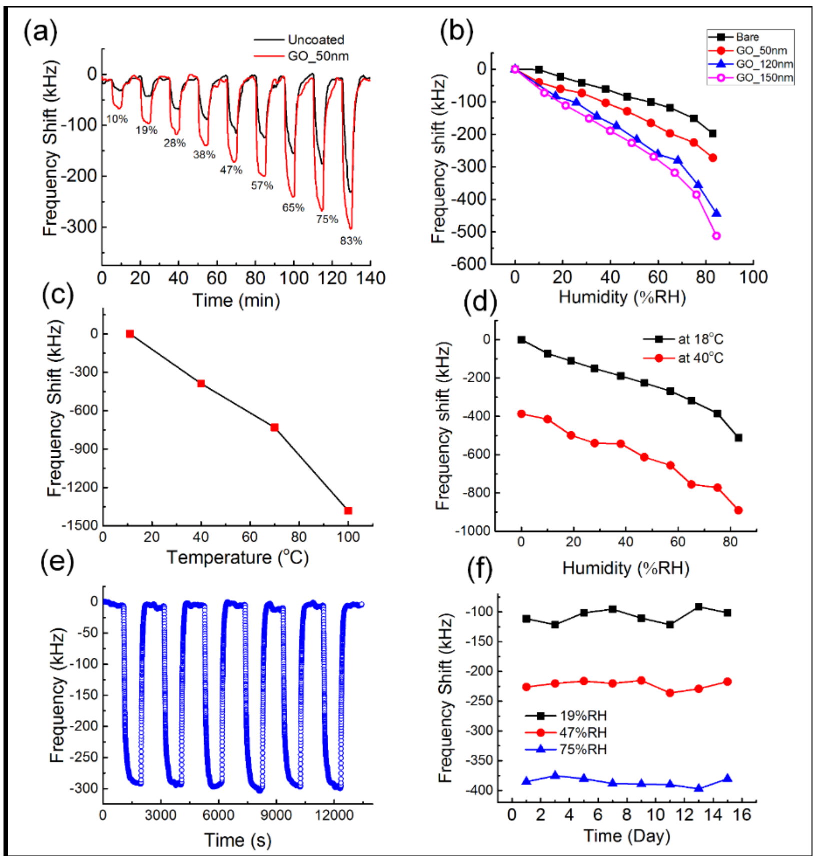

Figure 4. (a) the real-time frequency response of the humidity sensor showing the absorption-desorption process, (b) the frequency shift with different thickness GO film, (c) the temperature coefficient of the oscillator, (d) humidity responses at 18 and 40 ^{o}C respectively, (e) the repeatability of the humidity sensor when the humidity was switched between 5%RH and 83%RH, and (f) the long-term stability of the oscillator sensors.

The Van der Waals force is believed to be responsible for the bonding (absorption) between water molecules and GO which is a weak force, and the interaction is concentration-dependent and reversible. Increasing the thickness of the GO film will enhance the sensitivity as shown in figure 4(b), and the maximum frequency shift is 550 kHz at 83%RH for a GO thickness of 150 nm. However, the frequency shift per %RH in the range between 70%RH to 83%RH is larger than those below 70%RH, which means the mass loading is higher at higher humidity levels. Hydrogen bonds of water absorbed on the GO surface may contribute to the absorption of water molecules, increasing the absorption of water molecules.

There are many factors which may affect the performance of the FBAR sensors such as temperature, different gas composition and vibration etc. The humidity responses at 18 and 40 ^{o}C were measured to clarify the temperature effect on the performance of the sensors, with the results shown in figure 4(d). The frequency shifts vs. humidity spectra are almost in parallel, implying the sensor maintains a similar performance at different temperatures, i.e. the temperature has limited effect on the sensitivity. Deliberate vibration of the test chamber resulted noise spike in the spectrum, but did not change the sensitivity. Similarly introduction of air instead of nitrogen gas into the chamber was found to have no effect on the sensitivity of the oscillator sensor. The repeated frequency shift with relative humidity changing between 3%RH and 83%RH is shown in figure 4(e) with the temperature fixed at 25 ^{o}C. As it can be seen that the variation of frequency shift at the two humidity levels is less than 5%, demonstrating the very stable characteristics of the humidity sensors fabricated. The long-term stability (continuous measurement) of the oscillator sensor up to 17 days was assessed at three different humidity levels as shown in figure 4(f), showing excellent stability with fluctuation less than 10%.

The mass load on the FBAR device is associated with L2 and R2 in figure 5(a), representing the energy loss and added motional inductance, respectively[18]. In the equivalent circuit, the L2 element is related to the physical parameters of the resonator and added mass[19]:

$$L_2 = \frac{4 f_s L_m \rho_2 d_2}{\rho_0 v_0} \tag{6}$$

Where $f_s = \frac{1}{2\pi\sqrt{L_m C_m}}$, is the serial resonance frequency of the bare FBAR, ρ_2, d_2, ρ_0, v_0 are the density of the added mass density, the thickness of the added film, the density of the piezoelectric layer and the acoustic velocity of the piezoelectric layer, respectively. The oscillator works at the serial resonant frequency of the FBAR device[18], and

$$\frac{\Delta f_S}{f_{\ S}} = -\frac{\Delta L}{2L} \approx -\frac{L_2}{2L_m} = -\frac{\rho_2 d_2}{\rho_0 d_0} \tag{7}$$

This equation is another form of the classic Sauerbrey equation, indicates that the resonant frequency of an acoustic resonator is linearly related to the mass absorbed on the surface. To verify that the value of L2 has a linear relationship with the output frequency of the oscillator, a simulation based on the oscillator was conducted, with the result shown in figure 5(b). Conclusion could be obtained that the frequency shift is proportional to the induced inductance by the mass loading. At the humidity above 70%RH, the amount of water molecules absorbed on the GO film is not linearly related to the relative humidity, additional molecules absorbed by the hydrogen bonds of water contribute to the higher frequency shift as discussed above.

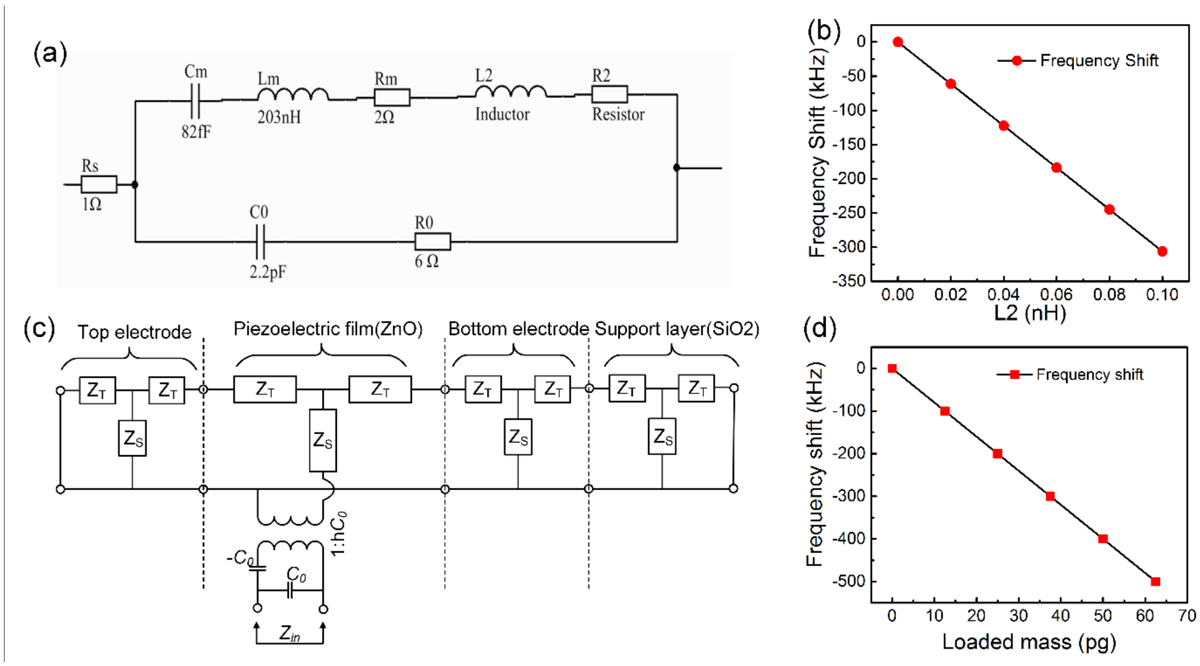

Figure 5. (a) the simulated relationship between the introduced inductor by the mass loading and the output frequency of the oscillator; (b) the MBVD model of FBAR device with mass loading, (c) the Mason's equivalent circuit of FBAR device , and (d) the theoretical frequency response of the FBAR based on Mason's model.

The simple MBVD equivalent circuit is useful in understanding the operation of a resonator, while in-depth analysis is necessary to further understand the mechanisms of a resonator such as the one-dimensional analytical model based on the transmission line wave theory[20, 21]. Since the thickness of the resonator is much smaller than the lateral dimensions, the Mason one dimension model is the most common one used to simulate the FBAR response. Figure 5(c) shows the schematic of the Mason's equivalent circuit of a FBAR device with the parameters expressed as follow:

$$Z = A\sqrt{\rho c_{33}^D}, \tag{8}$$

$$Z_T = jZtan(\frac{kd}{2}) \tag{9}$$

$$Z_S = -jZsin^{-1}(kd) \tag{10}$$

$$C_0 = \frac{e_{33}^S A}{d} \tag{11}$$

where ρ is the density of the layer material, d is the thickness of the layer, k is the wavenumber, e_{33}^S is the complex permittivity and c_{33}^D is the open circuit complex elastic stiffness, C_0 is the static capacitance,. The input impedance of the piezoelectric layer, Z_{in}, could obtained from the equivalent circuit in figure 5(c),

$$Z_{in} = \frac{1}{j\omega C_0}\left[1 - k_t^2 \cdot \frac{tan\theta}{\theta} \cdot \frac{\frac{Z_T+Z_S}{Z_0}cos^2\theta + jsin(2\theta)}{\frac{Z_T+Z_S}{Z_0}cos(2\theta) + j(1+\frac{Z_T Z_S}{Z_0^2})sin\,(2\theta)}\right] \tag{12}$$

where k_t^2 is the electromechanical-coupling coefficient, Z_0 is the characteristic impedance of the piezoelectric plate, Z_T and Z_S represents the acoustics loads at the two boundaries of the piezoelectric film from the +z and –z direction, $\theta = kd/2$ is the phase change across the piezoelectric film. If the resonator has no electrode and no mass load, $Z_T = Z_S = 0$, then,

$$Z_{in} = \frac{1}{j\omega C_0}(1 - k_t^2 \cdot \frac{tan\theta}{\theta}) \tag{13}$$

If the mass is distributed uniformly on the surface of the resonator, the parallel resonant frequency of the fundamental model of FBAR can be approximated by:

$$f_{load} = \frac{f_{unload}}{1+\frac{\rho_m d_m}{\rho_p d_p}} \tag{14}$$

where f_{unload} is the ideal parallel resonant frequency of unload FBAR, the sub index m refers to the loaded mass and index p refers to the piezoelectric film. Then the simulation model is built up as a functional block in the ADS software (Keisight Corporation), thickness of the added mass is utilized as a parameter, as shown in figure 5(d), the frequency response vs. the loaded mass.

Compared with the reported acoustic wave based humidity sensors, the sensitivity of the FBAR oscillator humidity sensor developed is higher than those of QCM sensors[22], but is comparable to or inferior to those of SAW humidity sensors [16] possibly due to the optimized FBAR device, oscillator and measurement conditions. However, the FBAR oscillator sensors has much smaller dimensions, and can be easily integrated with CMOS circuit, which can be difficult to realize for both QCM and SAW sensors. Furthermore, a frequency counter has been developed and used for sensing, instead of using a network analyzer for sensing. Both of them could enable the FBAR oscillator sensors to be integrated into any microsystem for practical application.

4. Conclusion

In this work, a FBAR Pierce oscillator and a FPGA based frequency counter were designed, simulated, and characterized. It has been used for humidity sensing with different thicknesses of graphene oxide sensing layer. The FBAR oscillator humidity sensor showed a linear relationship between the oscillating frequency shift and humidity at the humidity less than 70%, and excellent repeatability and stability. The absorption-desorption process was analyzed and it was shown that incorporation of GO layer enhances the humidity sensitivity up to 25.5 kHz/1%RH, demonstrated the potential application of integrated FBAR and CMOS circuit in electronic systems and portable devices which has high sensitivity, small dimensions and low power consumption.

Acknowledgment

This work was supported by NSFC (Nos. 61274037 and 61274123). W.P. Xuan thanks the financial support from Zhejiang University, The international research collaboration for PhD students. The authors thank Mr. Frank Courtney (Warwick University, UK) for his assistance in wire bonding.

References

[1] Rittersma Z M, Splinter A, Bodecker A and Benecke W 2000 A novel surface-micromachined capacitive porous silicon humidity sensor *Sens. Actuators, B* **68** 210-7

[2] Yoo K P, Lim L T, Min N K, Lee M J, Lee C J and Park C W 2010 Novel resistive-type humidity sensor based on multiwall carbon nanotube/polyimide composite films *Sens. Actuators, B* **145** 120-5

[3] Wang X, Ding B, Yu J, Wang M and Pan F 2010 A highly sensitive humidity sensor based on a nanofibrous membrane coated quartz crystal microbalance *Nanotechnol.* **21** 055502

[4] Yao Y and Xue Y J 2015 Impedance analysis of quartz crystal microbalance humidity sensors based on nanodiamond/graphene oxide nanocomposite film *Sens. Actuators, B* **211** 52-8
[5] Sheng L, Dajing C and Yuquan C 2011 A surface acoustic wave humidity sensor with high sensitivity based on electrospun MWCNT/Nafion nanofiber films *Nanotechnol.* **22** 265504
[6] Xuan W, He X, Chen J, Wang W, Wang X, Xu Y, Xu Z, Fu Y Q and Luo J K 2015 High sensitivity flexible Lamb-wave humidity sensors with a graphene oxide sensing layer *Nanoscale* **7** 7430-6
[7] Qiu X T, Tang R, Zhu J, Oiler J, Yu C J, Wang Z Y and Yu H Y 2010 Experiment and theoretical analysis of relative humidity sensor based on film bulk acoustic-wave resonator *Sens. Actuators, B* **147** 381-4
[8] Bi H, Yin K, Xie X, Ji J, Wan S, Sun L, Terrones M and Dresselhaus M S 2013 Ultrahigh humidity sensitivity of graphene oxide *Sci. Rep.* **3**
[9] Lu Y, Chang Y, Tang N, Qu H, Liu J, Pang W, Zhang H, Zhang D and Duan X 2015 Detection of Volatile Organic Compounds Using Microfabricated Resonator Array Functionalized with Supramolecular Monolayers *ACS Appl. Mater. Interfaces* **7** 17893-903
[10] Li M, Seok S, Rolland N, Rolland P, El Aabbaoui H, de Foucauld E, Vincent P and Giordano V 2014 Ultralow-phase-noise oscillators based on BAW resonators *IEEE Trans. Ultrason. Ferroelectr. Freq. Control.* **61** 903-12
[11] Otis B P and Rabaey J M 2003 A 300-mu W 1.9-GHz CMOS oscillator utilizing micromachined resonators *IEEE J. Solid-State Circuits* **38** 1271-4
[12] Pang W, Ruby R C, Parker R, Fisher P W, Unkrich M A and Larson J D 2008 A temperature-stable film bulk acoustic wave oscillator *Ieee Electr Device L* **29** 315-8
[13] Rai S S and Otis B P 2008 A 600 uW BAW-tuned quadrature VCO using source degenerated coupling *IEEE J. Solid-State Circuits* **43** 300-5
[14] Heragu A, Ruffieux D and Enz C 2013 A Low Power BAW Resonator Based 2.4-GHz Receiver With Bandwidth Tunable Channel Selection Filter at RF *IEEE J. Solid-State Circuits* **48** 1343-56
[15] Larson Iii J D, Bradley P D, Wartenberg S and Ruby R C 2000 Modified Butterworth-Van Dyke circuit for FBAR resonators and automated measurement system. IEEE) pp 863-8
[16] Xuan W, He M, Meng N, He X, Wang W, Chen J, Shi T, Hasan T, Xu Z, Xu Y and Luo J K 2014 Fast response and high sensitivity ZnO/glass surface acoustic wave humidity sensors using graphene oxide sensing layer *Sci. Rep.* **4** 7206
[17] Sauerbrey G 1959 Use of vibrating quartz for thin film weighing and microweighing *Z. Phys.* **155** 206-22
[18] Zhang H and Kim E S 2005 Micromachined acoustic resonant mass sensor *J. Microelectromech. Syst.* **14** 699-706
[19] Martin S J, Granstaff V E and Frye G C 1991 Characterization of a Quartz Crystal Microbalance with Simultaneous Mass and Liquid Loading *Anal. Chem.* **63** 2272-81
[20] Mason W P 1948 *Electromechanical transducers and wave filters*: D. Van Nostrand Co.)
[21] Mason W P 1956 Physical acoustics and the properties of solids *J. Acoust. Soc. Am.* **28** 1197-206
[22] Yao Y, Chen X D, Li X Y, Chen X P and Li N 2014 Investigation of the stability of QCM humidity sensor using graphene oxide as sensing films *Sens. Actuators, B* **191** 779-83